

Influence of Rheological Properties of Adhesive Polymer on Strain Energy Release Rate of Mode II and Adhesive Shear Strength

WON WOO LIM, HIROSHI MIZUMACHI

Division of Polymeric Materials, Department of Biomaterial Science, The University of Tokyo, 1-1-1 Yayoi, Bunkyo-ku, Tokyo 113, Japan

Received 7 January 1997; accepted 17 April 1997

ABSTRACT: It is well known that adhesive strength shows temperature and rate dependencies reflecting viscoelastic properties of an adhesive used. Specifically, a mechanical relaxation mechanism around the glass transition temperature (T_g) has a strong effect on the adhesive strength, which involves deformation of the adhesive layer. In addition, it is very interesting to know how viscoelastic properties of the adhesive affect the value of strain energy release rate since deformation and failure of the adhesive occur at the measurement of strain energy release rate for adhesive joints. In this study, adhesive tensile strength and strain energy release rate (G_{IIC}) in plain-shearing mode were measured under a constant experimental condition using adhesives consisting of two types of epoxy resins; the influence of viscoelastic properties on these two values was investigated, and we discuss the relationship between the adhesive shear strength and G_{IIC} . © 1997 John Wiley & Sons, Inc. *J Appl Polym Sci* **66**: 525–536, 1997

INTRODUCTION

Adhesives are polymeric materials. The mechanical properties of the materials vary with their chemical and supermolecular structures. Because linear viscoelastic functions, such as relaxation modulus, creep compliance, and complex modulus, change greatly according to temperature and time scale (i.e., deformation rate, frequency, and time), it is necessary to know whether a polymer is in a glassy, rubbery, or flowing state under any conditions by measuring the value of the functions. It is known that temperature and rate (time or frequency) superposition procedure holds for the linear viscoelastic functions over a wide range of temperatures and time scales, and a smooth master curve is obtained.^{1–3} The same procedure cannot be applied in a strict sense to the fracture

of polymeric materials because a large deformation, as well as initiation and propagation of the crack, are involved in the phenomena.

However, T. L. Smith⁴ has pointed out the fact that the temperature and rate superposition principle apparently holds for the data of stress and strain at failure of rubbers, which he obtained over a wide range of temperature and deformation rates (R). A master curve of failure stress (σ_B) plotted against $\log(1/R)$ is a sigmoid, and that of failure strain (ϵ_B) is a curve with a single peak. He also showed that the shift factor, $\log(a_T)$ in this case followed the Williams, Landel, and Ferry (WLF) equation. A general curve of σ_B plotted against ϵ_B was called the failure envelope. T. Hata⁵ explained qualitatively the characteristics of failure envelope in terms of a simple mechanical model and two failure criteria.

Adhesive strength is defined as a value of an external force (or stress) at failure, but its physical meaning is not necessarily clear because cohesive fracture of adhesive and adherend, interfacial fracture, and the mixed mode fractures occur in

Correspondence to: Won Woo Lim.

Table I Characteristics of the Adherend

Adherend	Specific Gravity		Moisture Content (%)	Young's Modulus E' ($\times 10^5$ kgf cm 2)
	Air	Dry		
Kaba	0.88	0.78	15	1.12

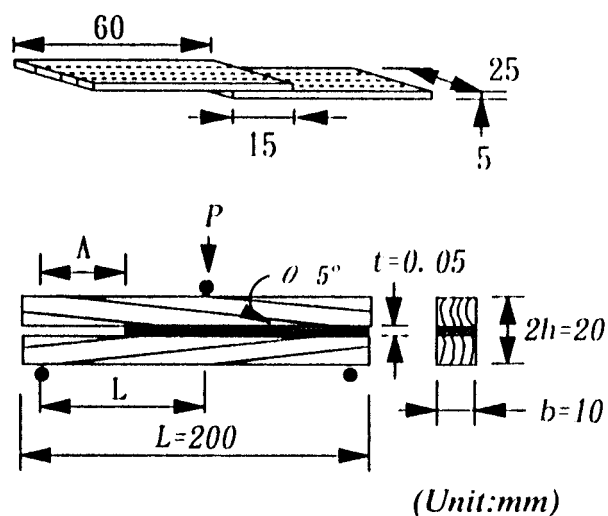
the adhesion tests. Nevertheless, it is sometimes pointed out that there is a correlation between the physical properties of a polymer and adhesive strength. Some try to understand temperature and rate dependencies of adhesive strength in relation to viscoelastic properties of adhesive.^{6,7} Hatanoto et al.⁸ measured adhesive tensile strength of cross-lap joints of wood bonded with epoxy resins and found that adhesive strength is very low when the modulus of the adhesive is either too high or too low, and a maximum value is obtained at around $E' = 1.0 \times 10^{10}$ dyne cm 2 . Similar behaviors were found also in the other adhesive joints.⁹⁻¹²

In many standards for testing materials, adhesive strength is defined as an external force to break the joints, which is divided by a bonding area or a width. When the external force is applied to the adhesive joints, complicated stress and strain distributions will generally be generated within the specimens, including the interface, adhesive layer, and adherend. Accordingly, a mechanical approach with an emphasis on the stress concentration is needed for adhesive joints in order to describe fracture behavior in terms of physically defined quantities. In fracture mechanics, stress concentration near the crack-tip of materials is related to the criteria of initiation and propagation of crack; and fracture toughness, K_C and G_C , are defined.

Mostovoy and Ripling^{13,14} studied fracture mechanics for aluminium-epoxy resins joints and confirmed that a strain energy release rate of adhesive joints could be measured easily if a proper shape and dimensions of a specimen are designed. Gent and Kinloch¹⁵ measured adhesive fracture energy (Φ) in mode II as a function of temperature and rate for copolymer of butadiene and styrene-mylar-coated steel joint and obtained a master curve by application of the WLF equation to the measured data. They also confirmed that energy criterion could be applied to the fracture of adhesive joints.

Chai¹⁶ also studied the fracture mechanical properties of steel specimens bonded with amorphous thermosetting resin and semicrystalline

thermoplastic resin and found that strain energy release rates for three modes of deformation, G_{IC} , G_{IIC} , and G_{IIIC} , depend upon a thickness (t) of the adhesive layer in different ways. A value of G_{IC} was constant independently of t , and both G_{IIC} and G_{IIIC} increased with an increase of t and then reached a plateau when t was over thickness (t_L). Lim et al.¹⁷⁻²⁰ studied fracture toughness of a series of wood-adhesive joints. First, they confirmed experimental conditions to estimate G_{IC} , G_{IIC} , and G_{IIIC} , which were not affected by the shape and dimension of the specimen. Second, they studied the temperature and rate dependencies of a strain energy release rate for typical adhesives. Third, they applied the temperature-rate superposition procedure to the obtained data in order to get a continuous master curve. They also examined the relationship between a strain energy release rate and adhesive strength. Finally, as a result of measuring adhesive tensile strength and $\sqrt{G_{IC}}$, they pointed out that both values showed the maximum at a viscoelastic condition of adhesives and the relationship between both values changed by viscoelastic properties of adhesives and a fracture type.

**Figure 1** Geometry of test specimens.

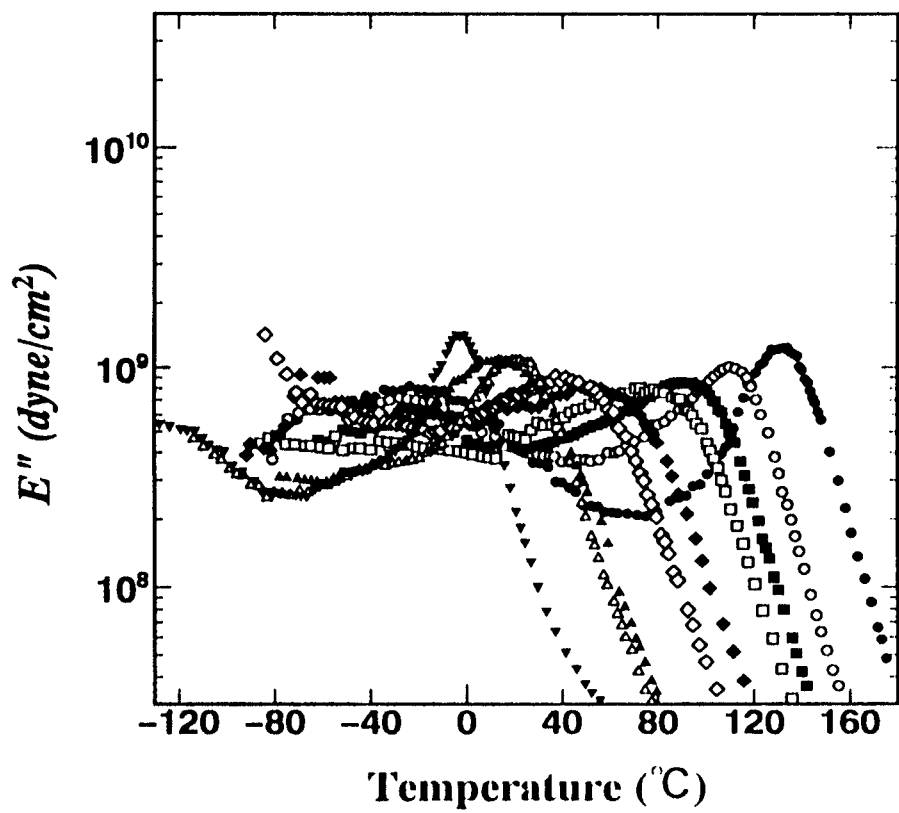
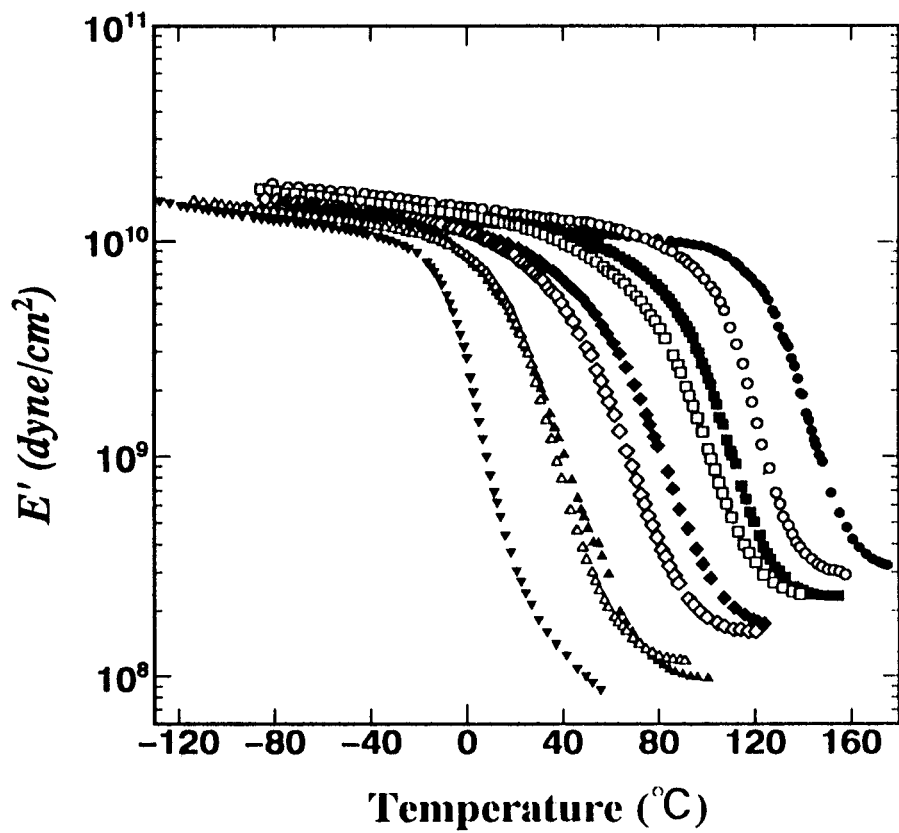


Figure 2

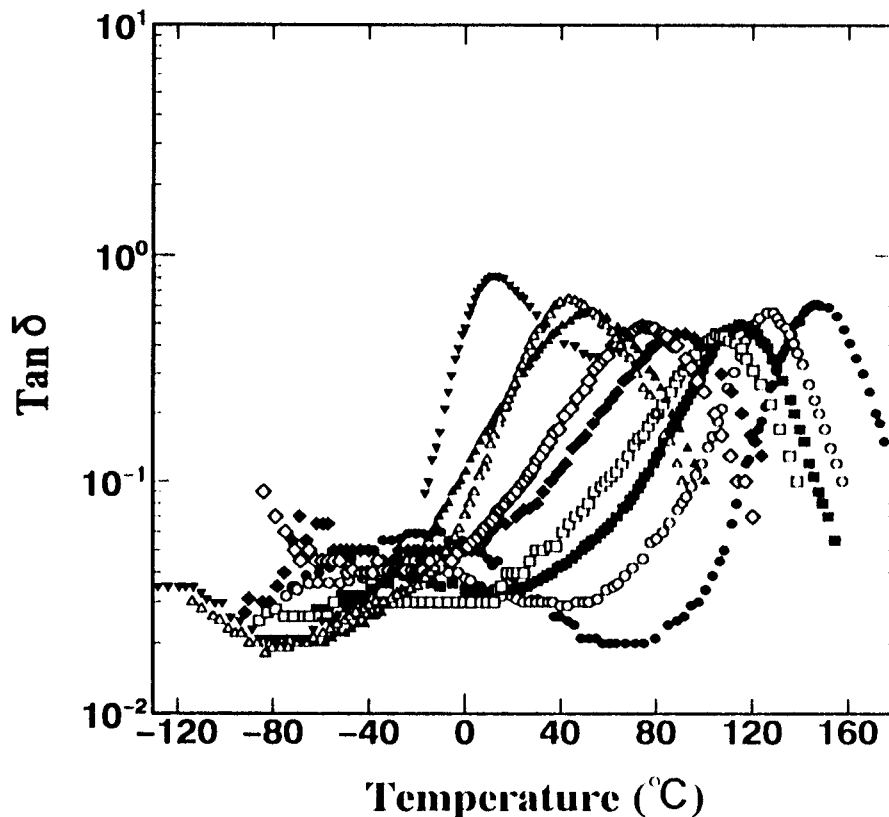


Figure 2 (Continued from the previous page) (a) Dynamic mechanical properties of cured films of adhesives: \circ , 0; \bullet , 0.2; \blacksquare , 0.3; \square , 0.4; \blacklozenge , 0.5; \diamond , 0.6; \blacktriangle , 0.7; \triangle , 0.8; \blacktriangledown , 1.0 (Epikote 871 : total epoxy). (b) Dynamic mechanical properties of cured films of adhesives: \circ , 0; \bullet , 0.2; \blacksquare , 0.3; \square , 0.4; \blacklozenge , 0.5; \diamond , 0.6; \blacktriangle , 0.7; \triangle , 0.8; \blacktriangledown , 1.0 (Epikote 871 : total epoxy). (c) Dynamic mechanical properties of cured films of adhesives: \circ , 0; \bullet , 0.2; \blacksquare , 0.3; \square , 0.4; \blacklozenge , 0.5; \diamond , 0.6; \blacktriangle , 0.7; \triangle , 0.8; \blacktriangledown , 1.0 (Epikote 871 : total epoxy).

In this study, we measured both a strain energy release rate (G_{IIC}) of the plain shearing mode and adhesive shearing strength using a series of epoxy resins with different glass transition temperatures. Also, we clarified the influence of viscoelasticity of adhesives on the correlation between the two values.

EXPERIMENTAL

Material

Adhesives used in this work are blends of two epoxy resins, Epikote 828 (Shell Chemical Co., Tokyo, Japan) and Epikote 871 (Shell Chemical Co., Tokyo, Japan). The blended epoxy resins are apparently transparent at room temperature. The adhesives are cured by adding a stoichiometric amount of diethylene tetramine (DETA) to the blends.

Japanese birch, Kaba (*Betula maximowiczana*

Regel), is used as an adherend, the physical properties of which are shown in Table I.

Measurement of Dynamic Mechanical Properties

The cured film was prepared by casting the mixture of Epikote 828 and Epikote 871, and DETA on a Teflon sheet, and keeping the mixture at room temperature and relative humidity (RH) of 65% for 5 days. Chemical structures of Epikote 828 and Epikote 871 were shown in Figure 1. The blend ratio of Epikote 871 : Epikote 828 ranged from 0 : 100 to 50 : 50, and the films were post-cured at 60–80°C for 2 h. Dynamic mechanical properties of the films were measured by means of a Rheovibron DDV-II (Toyo Baldwin Co., Ltd.) at 110 Hz with an average heating rate of 1°C min.

Measurement of Strain Energy Release Rate of Adhesive Joints

Wood specimens for fracture mechanical tests were prepared with grain angle of five degrees, as

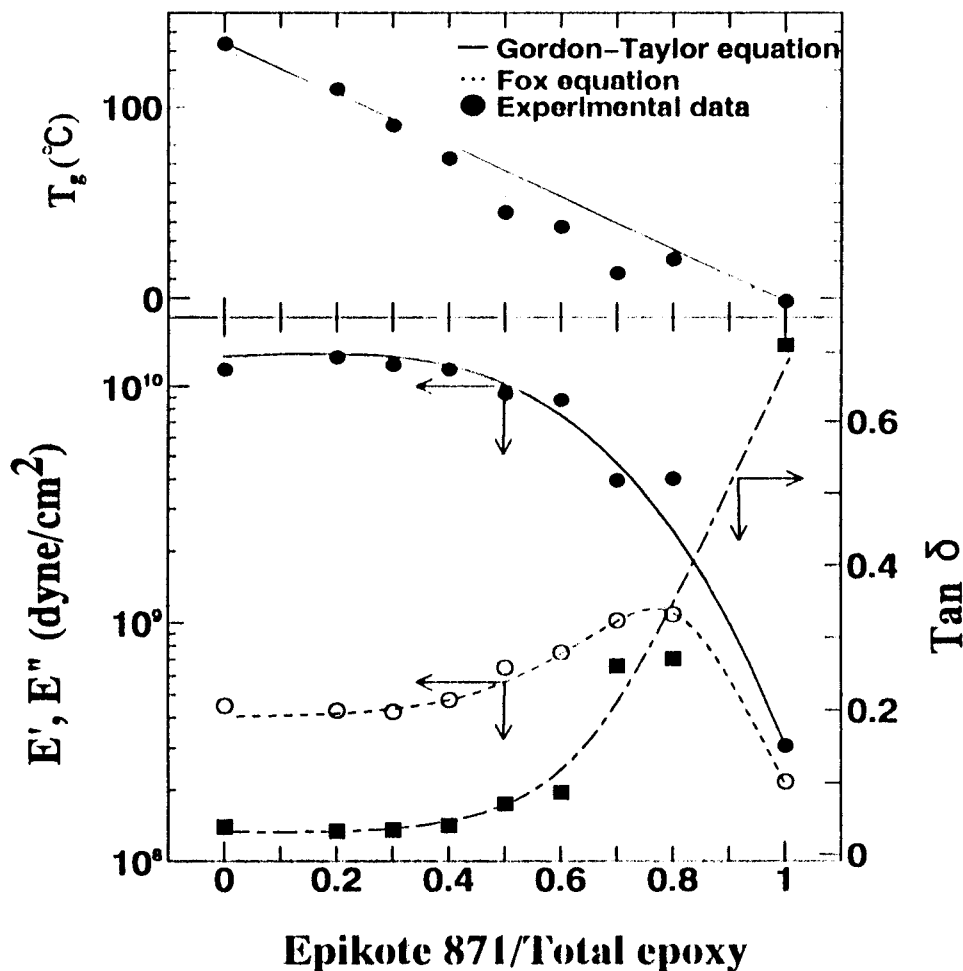


Figure 3 Glass transition temperature, E' , E'' , and $\tan \delta$ at room temperature with various blend ratios.

shown in Figure 1 in order to prevent wood failure along the grain. Pre-crack length was 4 cm, referring to our previous work.¹⁷ The amount of adhesive employed in this work was 250–300 g cm². As shown in Figure 1, the mode II fracture specimen test was the ENF (end notched flexure) test. Loading in the mode II test was the same as for a three-point bending test. For mode II specimens, a 0.05 mm thick Teflon strip was inserted into the crack.

The specimen was pressed under 10 kg cm² and was kept at 20°C and RH 65% for 4 days for curing. The bonded specimen were postcured at 60–80°C for 2 hrs. A fracture mechanical test was carried out with a crosshead speed of 10.0 mm min over a range of –60 to 80°C by means of Tensilon (Orientec Co., Tokyo, Japan). A strain energy release rate, G_{IIC} , was determined by the compliance method according to the following equation:

$$G_{IIC} = \frac{P_C^2}{2b} \left(\frac{\partial C}{\partial A} \right) \quad (1)$$

where P_C and E are failure load and Young's modulus of the adherend, respectively and the other parameters are shown in Figure 1.

Measurement of Adhesive Shear Strength

The specimen for the shear lap test was prepared as shown in Figure 1. The adhesion condition such as a spread amount of adhesive and bonding pressure was the same as that of the case of fracture mechanical test described above. The measurement of adhesive shear strength was carried out with the crosshead speed of 10.0 mm/min over a range of –60 to 80°C using Tensilon. The percentage of wood failure was visually observed.

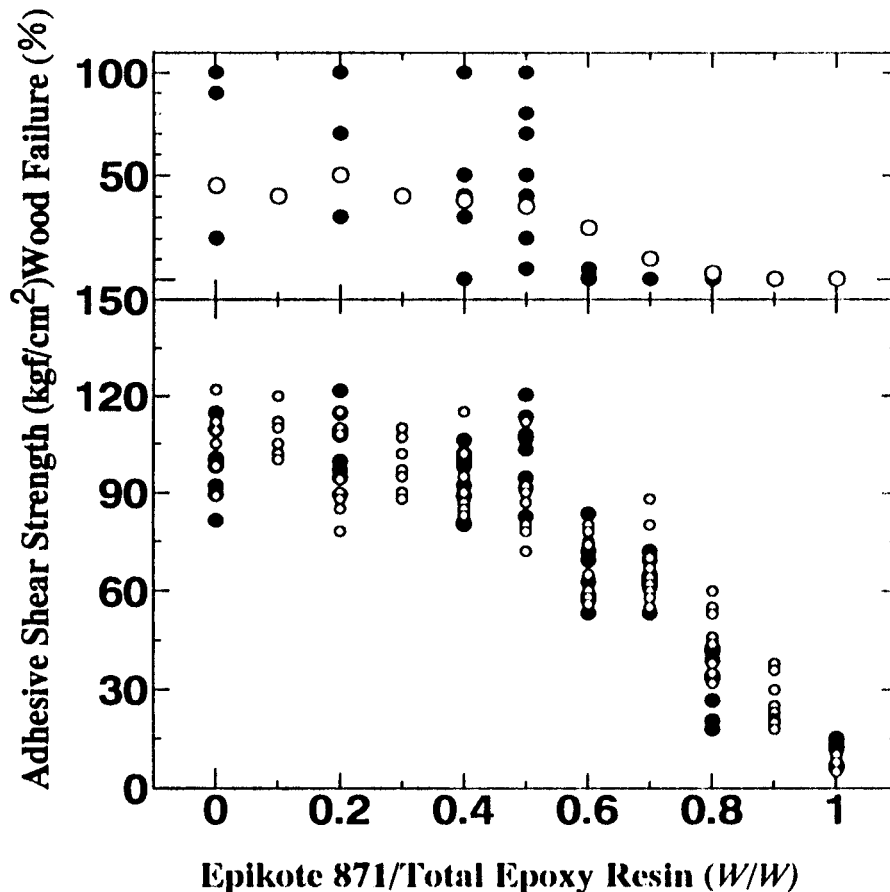


Figure 4 Dependence of adhesive shear strength of the blend ratio: ●, measured in this work; ○, measured by Y. Hatano in Kobayashi et al.¹² under the same conditions as in this work.

RESULTS AND DISCUSSION

Dynamic mechanical properties of cured films of adhesives are shown in Figure 2. When two types of epoxy resins, Epikote 871 and Epikote 828, were blended at various ratios and cured with a common hardner DETA, a series of polymers with different mechanical properties were obtained. Curves of storage modulus (E'), loss modulus (E''), and $\tan \delta$ plotted as a function of temperature were shifted toward high temperature as Epikote 828 content increased. That might suggest that the two epoxy compounds were mixed at a cured state to a considerable extent. However, there were cases where double peaks or shoulders were found in the E'' and $\tan \delta$ curves, especially in the intermediate blend ratios. Epikote 871 and Epikote 828 were molecularly miscible with each other in the liquid state. However, as the blends had been cured with DETA, a phase separation might have occurred

to some extent, although such phenomena had not been visualized in this study. Suzuki²¹ also pointed out the possibility of the phase separation in the same blend systems in his mechanical study on adhesive strength of scarf and butt joints where steel was bonded using the same adhesives.

Glass transition temperature, E' , E'' , and $\tan \delta$ at room temperature were plotted against the blend ratio in Figure 3. It is interesting to notice that T_g of the film changes almost linearly with a blend ratio. This trend can be described approximately in terms of either the Gordon-Taylor equation²² or the Fox equation,²³ which are derived for T_g of the miscible blends. Storage modulus at room temperature was almost constant when the Epikote 871 content was between 0 and 40% and decreased gradually as the content exceeded 40%. Loss modulus increased at first and then decreased through a maximum as Epikote 871 content increased or storage modulus de-

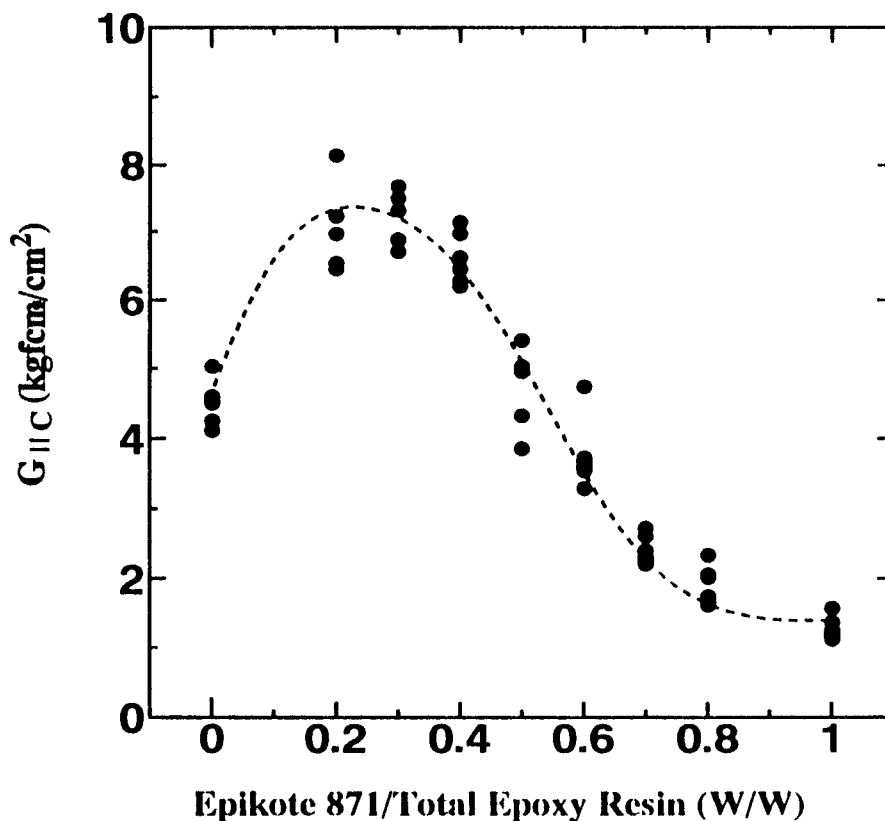


Figure 5 Dependence of G_{IIc} on the blend ratio.

creased. It was known that $\tan \delta$ was almost constant when the Epikote 871 content was between 0 and 40% but increased linearly when the content increased over 40%. From these facts, it was known that epoxy resins with various blend ratios used in this work were in a glassy state at room temperature when the Epikote 871 : Epikote 828 ratio was low, and then in a transient state, and in a rubbery state as the ratio increased. It was considered that these viscoelastic properties of adhesives would affect the adhesive strength and the strain energy release rate (G_C).

Figure 4 shows the dependence of adhesive shear strength on the blend ratio. The same figure included data obtained by Hatano et al.⁸ In cases in which Epikote 871 was low and the modulus of adhesives was high ($E' > 1.0 \times 10^{10}$ dyne cm²), adhesive shear strength was shown to be about 100 kgf cm². Also, failure, mixed with cohesive fracture of adherend and interfacial fracture, occurred. Adhesive shear strength decreased as the modulus of adhesives decreased with increasing Epikote 871 content. When the content of Epikote 871 was very high, adhesives were soft, and cohe-

sive strength became low. Accordingly, cohesive fracture of adhesives occurred. Wood failure was also naturally high. In the case of adhesive tensile strength, adhesive tensile strength showed a maximum when the modulus of adhesives was around 1.0×10^{10} dyne cm². However, this phenomenon was not found in the case of adhesive shear strength.¹⁹ When adhesive shear strength increased, wood failure was naturally high; but at the same time, there were much scatter of points. Hatano et al. described these facts in detail.⁸ A similar phenomenon was also found in other adhesive joints.⁹⁻¹²

Figure 5 shows the dependence of G_{IIc} on the blend ratio. G_{IIc} of adhesive joints bonded with Epikote 828-DETA was about 4.5 kgf cm². However, G_{IIc} increased with increasing Epikote 871 content and showed a maximum around the Epikote 871 content of 20%. The maximum value was approximately 7.0 kgf cm². This means that two epoxy blends were toughened by adding Epikote 871, which was a soft component, to Epikote 828, which was a hard component. When the Epikote 871 content increased further, the modulus and

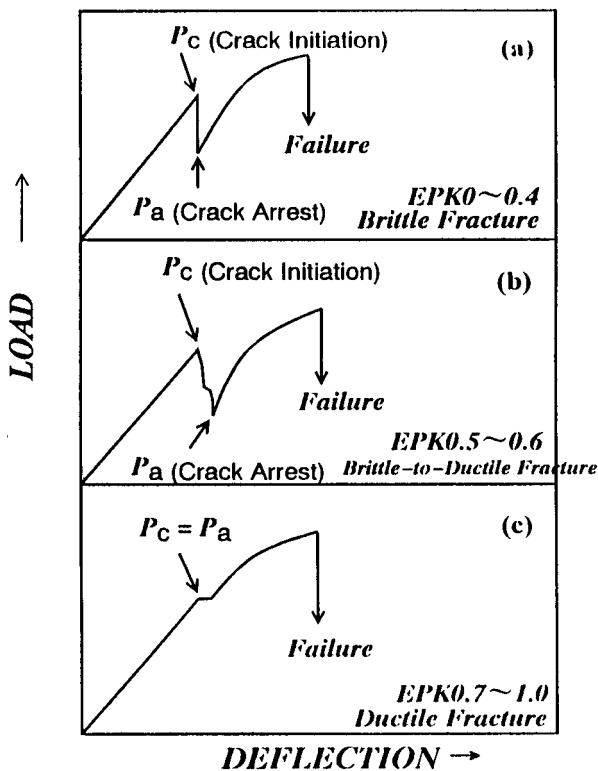


Figure 6 Stress-strain curves on fracture mechanical test with various blend ratios.

cohesive strength of adhesives decreased in order; and at the same time, G_{IIC} decreased because the resistance against crack propagation decreased.

Load displacement curves on fracture mechanical test changed, reflecting a change of viscoelastic properties of adhesives. Some typical examples are shown in Figure 6. When the Epikote 871 content was low and modulus of adhesives was high ($E' > 1.0 \times 10^{10}$ dyne cm^2), i.e., adhesives were in glassy state at room temperature, a typical unstable brittle fracture occurred, as shown in Figure 6(a). When the blending ratio was 50–60%, adhesives were in a transition state ($E' = 1.0 \times 10^{10}$ dyne cm^2) at room temperature; but a fracture type changed from brittle to ductile fracture in this state. In this case, the load displacement curve often showed unstable ductile fracture, as shown in Figure 6(b). As Epikote 871 content increased further, the modulus of adhesives became low, and a resistance against the external force at the crack tip decreased. Also, the load displacement curve showed ductile fracture, where a crack arrest mostly did not occur, as shown in Figure 6(c).

Both loads of crack propagation (P_c) and crack arrest (P_a) in the load displacement curves changed in order with the content of Epikote 871 : Epikote 828. Figure 7 shows P_a , P_c , and $(P_c - P_a)$ as a function of a blending ratio. When the Epikote 871 content was low and the modulus of adhesives was high, a brittle fracture occurred, but the value of $(P_c - P_a)$ was high. However, when the content was high and the modulus of adhesives was low, a ductile fracture occurred, and the value

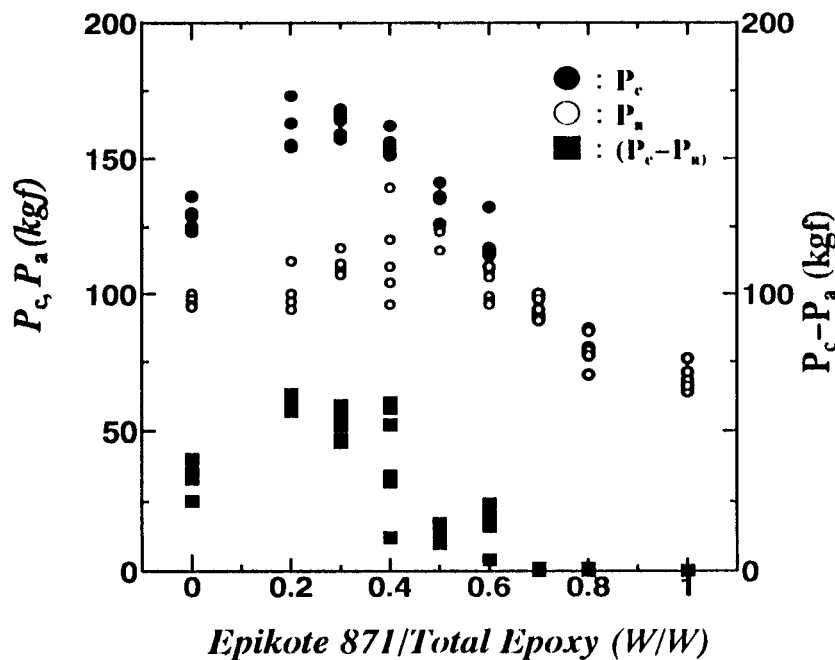


Figure 7 P_a , P_c , and $(P_c - P_a)$ as a function of blend ratio.

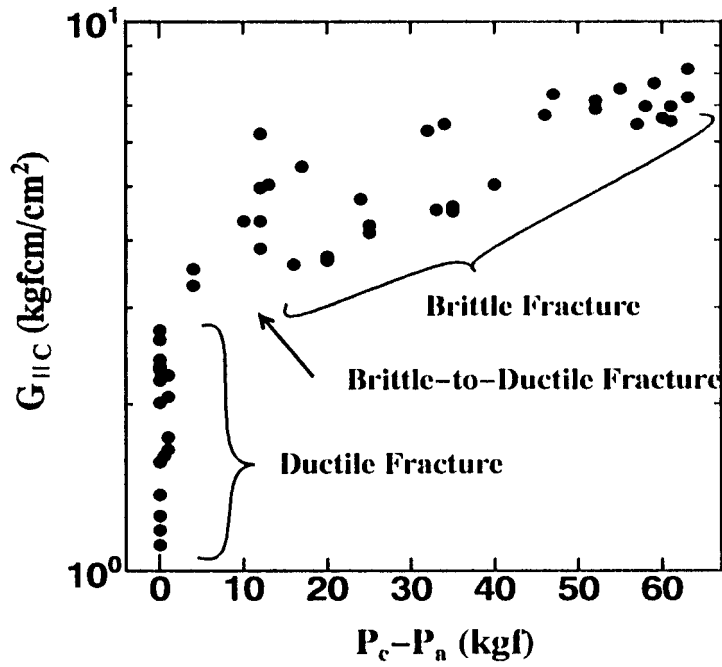


Figure 8 Plot of G_{IIc} against $(P_c - P_a)$.

of $(P_c - P_a)$ became near zero. When G_{IIc} was plotted against $(P_c - P_a)$, Figure 8 was obtained. When it was considered that the time from the crack

initiation to arrest was very short, $P_c - P_a$ was the same, meaning to speed up crack propagation. A positive correlation was found between G_{IIc} and

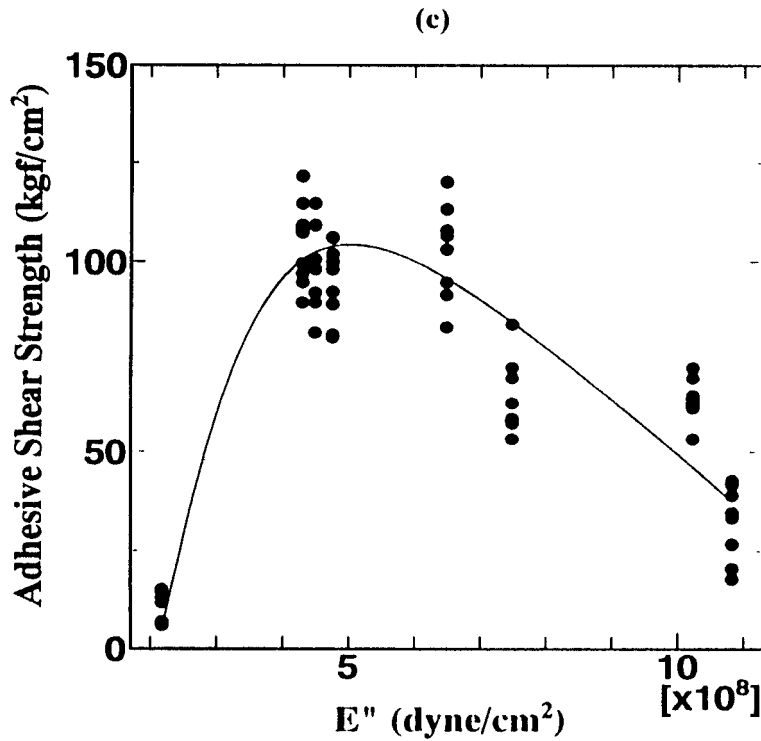


Figure 9 Dependence of adhesive shear strength upon ΔT , E' , E'' , and $\tan \delta$ at room temperature.

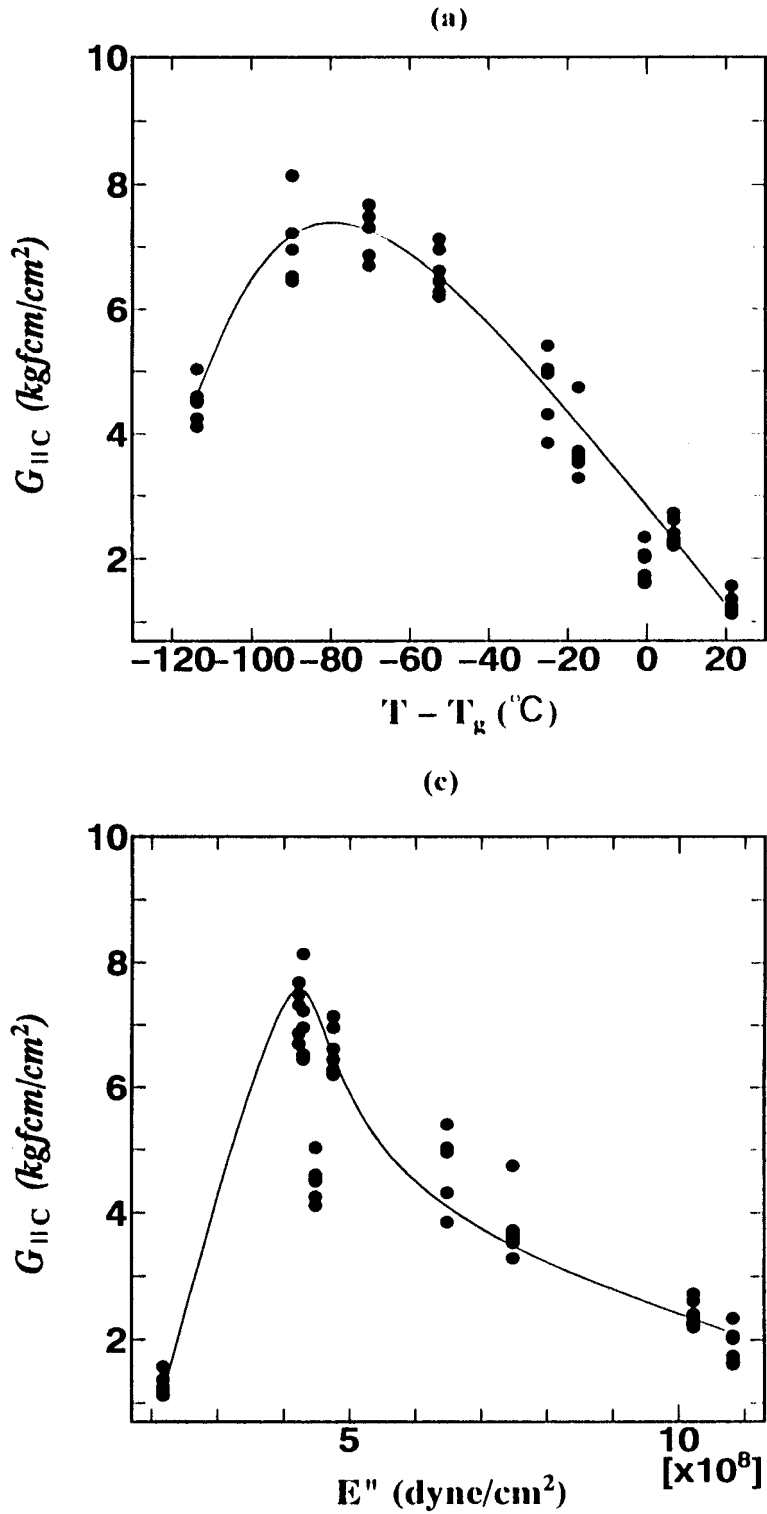


Figure 10 Dependence of G_{IIc} upon ΔT , E' , E'' , and $\tan \delta$ at room temperature.

$(P_c - P_a)$, except for $P_c - P_a = 0$, which was a perfect ductile fracture. Namely, it means that the speed of the crack propagation in the region of occur-

rence of the brittle fracture was high, but the speed was low by changing from brittle fracture to ductile.

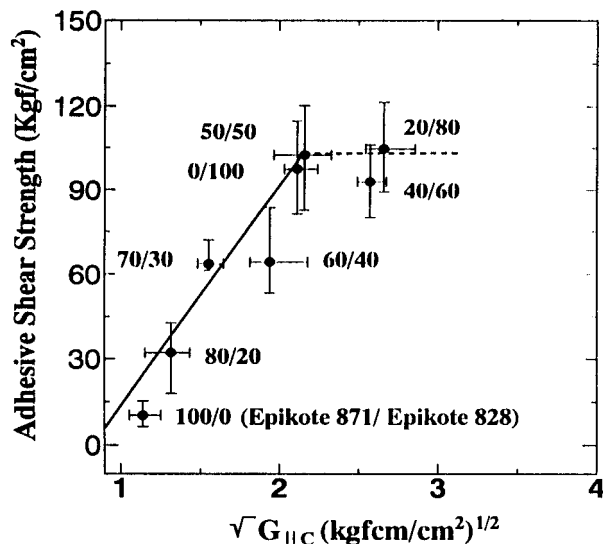


Figure 11 Relationship between adhesive shear strength and $\sqrt{G_{IIC}}$.

Figure 9 shows the dependence of adhesive shear strength upon ΔT ($= T - T_g$, T , and T_g are the room temperature and glass transition temperature, respectively), and E' , E'' , and $\tan \delta$ at room temperature. Adhesive shear strength was low when the T_g of adhesives was sufficiently lower than room temperature (experimental temperature) and increased with an increasing T_g . However, the strength did not show a maximum value like in the case of adhesive tensile strength, but had an almost constant value in the final results. This corresponded to the fact that the adhesive strength increased with increasing E' of adhesives and became a constant value in final. Because E' , E'' , and $\tan \delta$ at room temperature changed with the change of T_g of adhesives, each curve had a maximum or a peak. The figure shows that adhesive shear strength was a maximum, at approximately $E' = 1.0 \times 10^{10}$ dyne cm^2 , $E'' = 5.0 \times 10^8$ dyne cm^2 , and $\tan \delta = 0.1$.

Figure 10 shows similar plots for G_{IIC} . Almost the same qualitative trend could be confirmed for the dependence of G_{IIC} on viscoelastic properties of adhesives.

Figure 11 shows the relationship between adhesive shear strength and $\sqrt{G_{IIC}}$. A positive correlation, including some scatter of points, was found between the two values, except for a higher G_{IIC} region. When adhesives were in glassy state, cohesive fracture of the adherend occurred mostly in the adhesive strength test. On the other hand, interfacial fracture occurred in a fracture mechanical test. Because resistance against crack propa-

gation of adhesives was high, as $\sqrt{G_{IIC}}$ was very high, cohesive fracture of the adherend occurred mostly in an adhesive shear strength test. Accordingly, $\sqrt{G_{IIC}}$ increased, but adhesive shear strength was constant because the strength became nearly the strength of the adherend itself. One of the reasons for the scattering was due to the different wood failure between the two tests.

CONCLUSION

When Epikote 827 and Epikote 871 were blended with various ratios and cured with a common hardener, DETA, a series of polymers that ranged from a glassy to a rubbery state at room temperature were obtained. Adhesive shear strength and G_{IIC} of wood-adhesive joints bonded with these polymers were measured.

Adhesive shear strength and G_{IIC} became a maximum approximately at $T_g = 60-80^\circ\text{C}$, $E' = 1.0 \times 10^{10}$ dyne cm^2 , $E'' = 5.0 \times 10^8$ dyne cm^2 , and $\tan \delta = 0.1$.

A relationship between adhesive shear strength and $\sqrt{G_{IIC}}$ was changed with viscoelastic properties of adhesives. Positive correlation, including some scatter of points, was found between the two values, except for the higher G_{IIC} region. Also, the relationship was different to that between adhesive tensile strength and $\sqrt{G_{IIC}}$.

REFERENCES

1. F. Bueche, *Physical Properties of Polymer*, Wiley, New York, 1970.
2. J. D. Ferry, *Viscoelastic Properties of Polymer*, Wiley, New York, 1970, Chap. 11.
3. A. V. Tobolsky, *Properties and Structure of Polymer*, Wiley & Sons, 1960, Chap. 4.
4. T. L. Smith, *J. Polym. Sci.*, **32**, 99 (1958).
5. T. Hata, *Zairyo*, **17**, 322 (1968).
6. Y. Yamagishi, Y. Hatano, and H. Mizumachi, *Holzforchung*, **34**, 169 (1980).
7. K. Taki, B. Tomita, and H. Mizumachi, *Mokuzai Gakkaishi*, **28**, 143 (1982).
8. Y. Hatano, B. Tomita, and H. Mizumachi, *Mokuzai Gakkaishi*, **29**, 578 (1983).
9. H. Mizumachi, Y. Hatano, and Y. Yamagishi, *Holzforchung*, **34**, 169 (1991).
10. L. D. Turreda, Y. Hatano, and H. Mizumachi, *Holzforchung*, **45**, 371 (1991).
11. K. Motohashi, B. Tomita, and H. Mizumachi, *Wood Fiber Sci.*, **16**, 72 (1984).

12. T. Kobayashi, Y. Hatano, and H. Mizumachi, *Mokuzai Gakkaishi*, **37**, 331 (1991).
13. S. Mostovoy and E. J. Ripling, *J. Appl. Polym. Sci.*, **13**, 1083 (1969).
14. S. Mostovoy and E. J. Ripling, *J. Appl. Polym. Sci.*, **15**, 661 (1971).
15. A. N. Gent and A. J. Kinloch, *J. Appl. Polym. Sci., Part A2*, **9**, 659 (1971).
16. H. Chai, *Int. J. Frac.*, **37**, 137 (1988).
17. W. W. Lim, Y. Hatano, and H. Mizumachi, *J. Appl. Polym. Sci.*, **52**, 967 (1994).
18. W. W. Lim and H. Mizumachi, *J. Appl. Polym. Sci.*, **57**, 55 (1995).
19. W. W. Lim and H. Mizumachi, *J. Appl. Polym. Sci.*, **63**, 835–841 (1997).
20. W. W. Lim and H. Mizumachi, *Kor. J. Rheol.*, **8**, 129–138 (1996).
21. Y. Suzuki, *Trans. Jpn. Soc. Mech. Eng.*, **50**, 926 (1985).
22. M. Gordon and J. S. Taylor, *J. Appl. Chem.*, **2**, 493 (1952).
23. T. G. Fox, *Bull. Am. Phys. Soc.*, **1**, 123 (1956).
24. H. Mizumachi, *J. Rub. Soc. Jpn.*, **62**, 488 (1989).